



NJC

Fluorescent Nanoparticle Sensors with Tailor-Made Recognition Units and Proximate Fluorescent Reporter Groups

Journal:	<i>New Journal of Chemistry</i>
Manuscript ID	NJ-LET-03-2018-001139.R1
Article Type:	Letter
Date Submitted by the Author:	01-May-2018
Complete List of Authors:	Xing, Xiaoyu; Iowa State University, Department of Chemistry Zhao, Yan; Iowa State University, Department of Chemistry

SCHOLARONE™
Manuscripts



Journal Name

COMMUNICATION

Fluorescent Nanoparticle Sensors with Tailor-Made Recognition Units and Proximate Fluorescent Reporter Groups

Xiaoyu Xing and Yan Zhao^{*a}Received 00th January 20xx,
Accepted 00th January 20xx

DOI: 10.1039/x0xx00000x

www.rsc.org/

The molecular recognition unit of a fluorescent sensor is its most cumbersome part to design and synthesize, but is key to the specificity of the sensor. Molecular imprinting within cross-linked micelles using easily synthesized modular templates allowed us to create analyte-specific binding sites with a nearby fluorescent probe. This strategy makes it straightforward to vary the recognition unit independent of the reporting unit, making the sensor potentially applicable to a wide range of molecular analytes.

Fluorescent sensors have attracted many researchers' attention for their high sensitivity, ease of operation, and broad range of analytes that can be detected.¹⁻⁶ The general design of a fluorescent sensor consists of a recognition unit whose binding of the analyte is transduced to a nearby fluorescent probe.⁷ Although different signal-transducing mechanisms such as quenching, FRET, and PET may be used, the central feature for any sensor is the selective binding of the interested analyte. With the advancement of supramolecular chemistry over the last decades, many metal-binding ligands and macrocycles have been developed and used in fluorescent sensing.^{1-5, 7} For molecular analytes, their structural diversity makes it challenging to have a common recognition motif. Generally speaking, the design and synthesis of the recognition unit in a fluorescent sensor is the most tedious part of the research and must be performed on an individual basis for each analyte.

Molecular imprinting is a technique to create analyte-specific binding sites in a polymer matrix.^{8, 9} Molecularly imprinted polymers (MIPs) have been used in molecular sensing since their discovery.¹⁰⁻¹⁷ Nonetheless, traditional MIPs are highly cross-linked macroscopic polymers with poor solubility and a heterogeneous distribution of binding sites. Although they can be converted into fluorescent sensors for specific molecules, their insolubility and high cross-linking density make

it difficult to manipulate these materials accurately on the molecular level.

In this work, we employed a strategy that combined covalent imprinting with post-functionalization on molecularly imprinted nanoparticles (MINPs).¹⁸⁻²¹ The strategy was enabled by the solubility of the materials in water and selected organic solvents, the nanodimension of the materials, and the location of the template near the surface of the cross-linked nanoparticles. Our method readily afforded a tailor-made binding site for specific analytes (carboxylic acids as an example) with a nearby fluorescent reporting probe. We believe the method represents a general way to construct molecule-specific fluorescent sensors with minimal individual design of the molecular recognition unit.

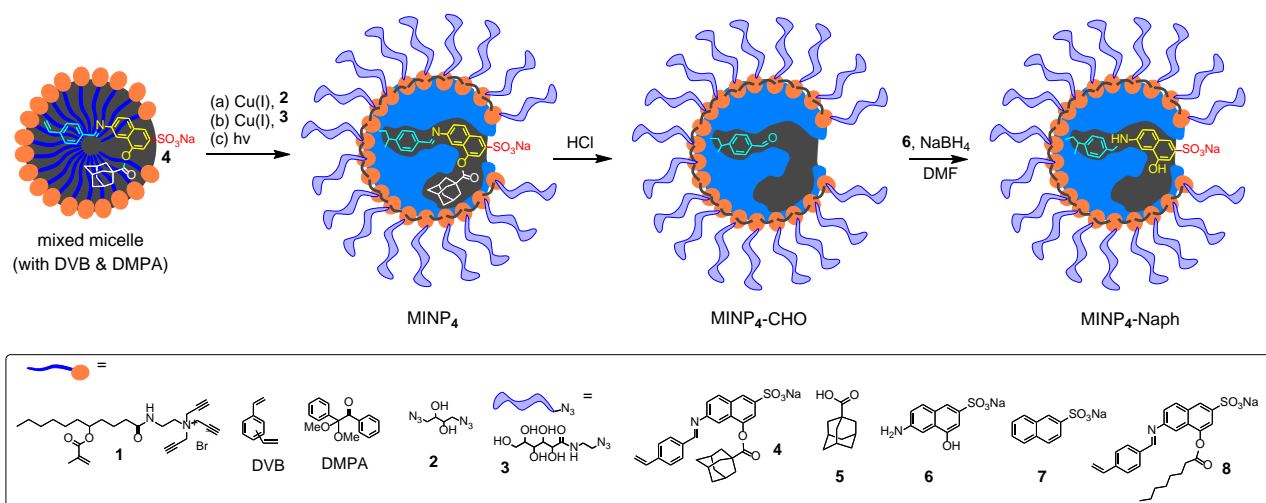
The synthesis of our fluorescent sensors is shown in Scheme 1, based on the micellar imprinting recently developed by our group.²²⁻²⁵ The essence of the method is to confine the polymerization/cross-linking for the imprinting within individual micelles, a feature that had been difficult to realize. Using the highly efficient click reaction between terminal alkyne and azide, we cross-linked the micelle of **1** first on the surface using diazide **2**. Another round of click reaction with monoazide **3** decorated the surface with a layer of hydrophilic groups.

The color-coded **4** in the mixed micelle of Scheme 1 is the key to our design. The molecule contains several "modules" that could be exchanged readily. The white-colored adamantanecarboxyl moiety is used to create an analyte-specific binding site (for 1-adamantanecarboxylic acid **5**). It is linked to the yellow fluorescent reporter that has a 6-aminonaphthalene-2-sulfonate moiety, which is similar to the more popular environmentally sensitive fluorophore dansyl (1-dimethylaminonaphthalene-5-sulfonyl). The amine group is linked by an imine bond to 4-vinylbenzaldehyde (shown in cyan). Previously, we have used an *ortho*-nitrobenzyl ester-based template and, by cleaving the photocleavable group, installed a carboxylic acid group inside the MINP binding pocket.²⁴ We chose an imine linkage in this work because of its

^a Department of Chemistry, Iowa State University, Ames, Iowa 50011-3111, USA.

Fax: +1-515-294-0105; Tel: +1-515-294-5845; E-mail: zhaoy@iastate.edu.

Electronic Supplementary Information (ESI) available: Experimental details, fluorescence titration curves, and additional data. See DOI: 10.1039/x0xx00000x



Scheme 1. Preparation of MINP-CHO by micellar covalent imprinting and hydrolysis, followed by reaction with **5** to re-form MINP(**4**).

much easier synthesis and facile post-functionalization (vide infra). The (red) anionic sulfonate group of **4** allowed the overall hydrophobic molecule to be easily incorporated into the cationic micelle of **1** and helped the molecule stay near the surface of the micelle. This feature is important to the hydrolysis of imine and the subsequent post-functionalization (vide infra).

As shown in Scheme 1, the mixed micelle also contained divinylbenzene (DVB) and 2,2-dimethoxy-2-phenylacetophenone (DMPA), which allowed us to perform photopolymerization/cross-linking of the micelle core, with **4** covalently attached to the micelle in the meantime by the free radical polymerization.

The synthesis and characterizations of MINPs have been reported previously²²⁻²⁵ and are found in the ESI. The surface-cross-linking, surface-decoration, and core-cross-linking were monitored by ¹H NMR spectroscopy and dynamic light scattering (DLS). DLS allowed us to measure the size of the MINP (ca. 5 nm) and estimate its molecular weight (ca. 50,000–60,000). The DLS size has been confirmed by transmission electron microscopy (TEM).^{26, 27}

With MINP₄ (i.e., MINP prepared with compound **4**) in hand, we studied different methods to hydrolyze the imine bond. Although the imine was located inside the hydrophobic core of the cross-linked micelle, 6 M HCl at 95 °C was found to cleave the fluorescent naphthyl group (along with the adamantyl). The naphthyl group emitted at 405 nm (Fig. S10). Treatment with the acid reduced the fluorescence intensity and the emission of the naphthyl disappeared nearly completely at 120 min (Fig. 1a, green spectrum).

At this point, the MINP₄-CHO produced is expected to contain voids left from the naphthyl and the adamantyl groups. The nanosized nanoparticle was soluble in DMF²⁴ and was mixed with a large excess (50 equiv) of 6-amino-4-hydroxy-2-naphthalenesulfonate **6** for 2 h. Formation of the imine bond was evident from the reappearance of the naphthyl emission after excess **6** was removed (compare the blue vs green spectra in Fig. 1a). However, the imine bond was not stable in aqueous solution, as incubation of the resulting nanoparticle (referred to

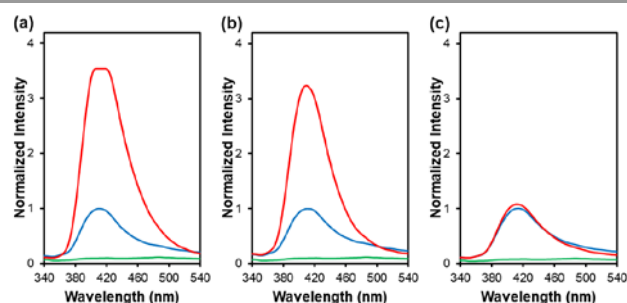


Fig 1. Normalized fluorescence spectra of MINP₄-CHO (green), as prepared MINP₄-C=N-Naph (blue), and MINP₄-C=N-Naph treated with (a) 0 equiv, (b) 100 equiv, (c) 500 equiv NaBH₄ (red). The red spectra were taken after the aqueous sample (blue spectrum) was left standing overnight. [MINP] = 5.0 μM. λ_{ex} = 307 nm.

as MINP₄-C=N-Naph) in water released **6** into the environment, which showed a stronger fluorescence (red).

Treatment of MINP₄-C=N-Naph with 100 equiv NaBH₄ increased its aqueous stability, as shown by the smaller difference between the incubated (red) and the as prepared MINP₄-C=N-Naph (blue) spectra in Fig. 1b. This should come from the reduction of the imine bond to amine by NaBH₄. Indeed, treatment of MINP₄-C=N-Naph with 500 equiv NaBH₄ led to aqueous-stable MINP₄-Naph that displayed little change in fluorescence after incubation in water overnight (Fig. 1c, note the nearly identical blue and red spectra).

If the hydrolysis of imine and the following reductive amination worked as expected, MINP₄-Naph was expected to have an adamantyl-shaped binding pocket with a nearby fluorescent group (Scheme 1). It should be able to bind 1-adamantanecarboxylic acid **5** and the binding should influence the fluorescence of the nearby covalently attached 6-aminonaphthalene-2-sulfonate. Indeed, as shown in Fig. 2, addition of **5** to an aqueous solution of MINP₄-Naph increased the latter's emission intensity steadily. The fluorescence increase was consistent with displacement of water molecules

near the probe by a more hydrophobic guest. The emission intensity fit well to a 1:1 binding isotherm, yielding a binding constant of $K_a = (48 \pm 14) \times 10^5 \text{ M}^{-1}$ (Fig. 2b). The 1:1 binding resulted from the 50:1 ratio used between **1** and **4**, as well as the aggregation number of the surfactant in the micelle (ca. 50).²² This feature has been verified numerous times in our previous MINPs both by fluorescence titration and isothermal titration calorimetry (ITC).²²⁻²⁵

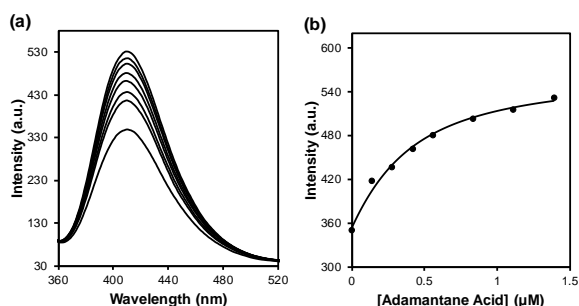


Fig 2. (a) Emission spectra of MINP₄-Naph upon addition of different concentrations of **5** in water. [MINP₄-Naph] = 1.0 μM. λ_{ex} = 307 nm. (b) Nonlinear least squares curve fitting of the fluorescence intensity at 410 nm to the 1:1 binding isotherm.

1-Adamantanecarboxylic has poor solubility in water. Its large hydrophobic surface area gives the molecule a strong driving force to enter a hydrophobic environment. Additionally, hydrogen bonds may form between the carboxylic acid of **5** and the hydroxyl group on the naphthyl group of MINP₄-Naph. The strong binding was consistent to the successful creation of the binding pocket from the covalent molecular imprinting and post treatment.

In our studies, we assumed the hydrolysis and reductive amination both proceeded quantitatively with the large excess of reagents used. Completion of the hydrolysis was evident from the near flat baseline of the fluorescence spectrum of MINP₄-CHO (Fig. 1, green spectra). The yield of the reductive amination, however, could not be determined directly. If the yield was less than quantitative, some of the binding events that occurred would not be reported by the fluorescence titration, as the fluorescent reporter would be absent in those MINPs that had not been functionalized with **6**. In such a case, the binding constant obtained from the fluorescence titration should represent the lower limit of the real value.

We are interested in detecting the acid in neutral water. When we performed the titration in 10mM HEPES buffer (pH 7.4), the binding was weaker, with $K_a = (3.0 \pm 0.3) \times 10^5 \text{ M}^{-1}$ (Fig. S13). This was a reasonable result because once the acid was deprotonated in the buffer, the ionic group would have difficulty entering a highly hydrophobic binding pocket due to the poor solvation of the carboxylate. The binding then needed to overcome an unfavorable re-protonation step, which weakens the binding.²⁴

To make sure our hydrolysis and reductive amination conditions did not damage the rest of the MINP structure, at least the binding site, we prepared a MINP receptor for naphthalenesulfonate **7**. This template does not have a

Table 1. Binding data for MINP₄-Naph and MINP₈-Naph for different acids in water.^a

Entry	MINP	Guest	$K_a (\times 10^5 \text{ M}^{-1})$	K_{rel}
1	MINP ₄ -Naph	5	48 ± 14	1
2	MINP ₄ -Naph	benzoic acid	2.8 ± 0.2	0.06
3	MINP ₄ -Naph	3,5-dinitrobenzoic acid	4.3 ± 1.2	0.09
4	MINP ₄ -Naph	butyric acid	0.20 ± 0.07	0.004
5	MINP ₄ -Naph	hexanoic acid	0.19 ± 0.05	0.004
6	MINP ₄ -Naph	octanoic acid	0.173 ± 0.006	0.004
7	MINP ₄ -Naph	decanoic acid	0.14 ± 0.03	0.003
8	MINP ₄ -Naph	lauric acid	~0.001 ^b	~0
9	MINP ₈ -Naph	octanoic acid	0.84 ± 0.14	1
10	MINP ₈ -Naph	acetic acid	-- ^c	~0
11	MINP ₈ -Naph	butyric acid	-- ^c	~0
12	MINP ₈ -Naph	hexanoic acid	-- ^c	~0
13	MINP ₈ -Naph	decanoic acid	~0.01 ^b	~0.01
14	MINP ₈ -Naph	lauric acid	~0.04 ^b	~0.05
15	MINP ₈ -Naph	5	~0.01 ^b	~0.01

^a The titrations were generally performed in duplicates and the errors between the runs were <10%. K_{rel} is the binding constant of a guest normalized to that of the targeted analyte by the same MINP receptor. ^b The titration showed very weak binding and the binding constant was estimated. ^c The fluorescence titrations showed random and negligible change.

polymerizable group and the imprinting is thus noncovalent in nature. We have shown anionic hydrophobic guests of similar size can be used effectively to create a template-specific binding pocket.^{22, 24, 25} In our hands, MINP₇ was found to bind **7** with $K_a = (6.2 \pm 0.2) \times 10^5 \text{ M}^{-1}$. After the 6M HCl treatment and “reductive amination/dialysis” (even though no imine bond was present), the MINP was found to bind **7** with $K_a = (5.7 \pm 0.6) \times 10^5 \text{ M}^{-1}$ and $(7.8 \pm 0.3) \times 10^5 \text{ M}^{-1}$, respectively (Fig. S14–S16). Thus, these treatments did not alter the binding properties of amine-free MINPs, suggesting the “backbone” structure of the MINP—comprising mainly hydrocarbon and cross-linked DVB/styrene/methacrylate—was not affected by the hydrolysis and reductive amination treatments.

One of the most important requirements for a sensor is its selective binding of the analyte among structural analogues. MINP₄-Naph showed significant selectivity for the targeted 1-adamantanecarboxylic acid. Its binding for other cyclic (benzoic and 3,5-dinitrobenzoic acid) and acyclic acids (C4–C12 linear carboxylic acids) were much lower, with the normalized binding constant (K_{rel}) ranging from 0–9% relative to that of the template itself (Table 1, entries 2–8). When 1.0 μM of different acids were added to the MINP sensor, the largest change in emission occurred with 1-adamantanecarboxylic (**5**) while other acids displayed much smaller changes (Fig. S31).

The homologous C2–C12 carboxylic acids differ only in their hydrocarbon chain length but have the same functional group. Although fluorescent sensors for carboxylic acids have been reported,²⁸⁻³⁰ distinguishing the chain length is very challenging because the carboxylic acid tends to be a better handle from the supramolecular point of view.

Our micellar molecular imprinting easily solved the above problem, using molecule **8** as the template that has an octanoate side chain. As expected, MINP₈-Naph was able to

bind octanoic acid, with $K_a = (0.84 \pm 0.14) \times 10^5 \text{ M}^{-1}$ (Table 1, entry 9). This value is about 1/60 of that for 1-adamentanecarboxylic acid by MINP₄-Naph (entry 1). The weaker binding is anticipated from the lower hydrophobicity of octanoic acid that gives a smaller driving force for the analyte to enter the MINP binding pocket.

Most importantly, MINP₈-Naph exhibited an excellent selectivity among the carboxylic acid homologues, shown by their very different binding constants (Table 1, entries 10–14).³¹ The distinction of the carbon-carbon chain length was quite remarkable, as either increasing or decreasing the carbon chain length shut off the binding nearly completely. Since the binding pocket of MINP₈-Naph is expected to be linearly C8-shaped, it is no surprise at all that 1-adamentanecarboxylic acid **5** could not fit in (entry 15).³²

The strong binding in water for the targeted hydrophobic acids (**5** and octanoic acid) translate to a fairly sensitive detection. The detection limits for the two acids were calculated to be 0.20 and 3.54 μM , respectively based on the $3\delta/\text{slope}$ (ESI).

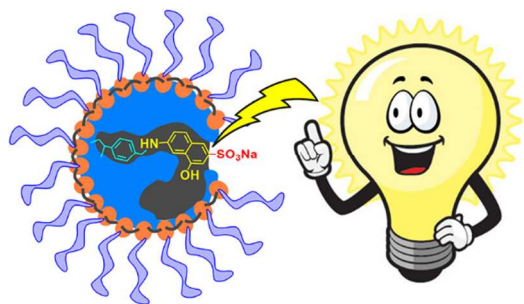
In summary, we have demonstrated a highly modular synthesis of imprinted fluorescent sensors. Although carboxylic acids are used to prove the concept, the method is general and should be applicable to other molecular analytes. Our method allows one to create an analyte-specific binding site with a nearby environmentally sensitive fluorescent probe. Our MINPs have been shown to detect peptides with very similar side chains,^{26, 27, 33} as well as mono- and oligosaccharides.^{34, 35} Integration of the fluorescent sensing mechanism demonstrated in this work potentially can afford selective sensors for many important biomolecules.

We thank NSF (CHE-1708526) for supporting this research.

Notes and references

1. B. Wang and E. V. Anslyn, *Chemosensors: principles, strategies, and applications*, Wiley, Hoboken, N.J., 2011.
2. V. M. Mirsky and A. K. Yatsimirsky, *Artificial receptors for chemical sensors*, Wiley-VCH Verlag, Weinheim, Germany, 2011.
3. E. M. Nolan and S. J. Lippard, *Chem. Rev.*, 2008, **108**, 3443-3480.
4. E. L. Que, D. W. Domaille and C. J. Chang, *Chem. Rev.*, 2008, **108**, 1517-1549.
5. K. P. Carter, A. M. Young and A. E. Palmer, *Chem. Rev.*, 2014, **114**, 4564-4601.
6. L. Y. Niu, Y. Z. Chen, H. R. Zheng, L. Z. Wu, C. H. Tung and Q. Z. Yang, *Chem. Soc. Rev.*, 2015, **44**, 6143-6160.
7. A. P. de Silva, H. Q. N. Gunaratne, T. Gunnlaugsson, A. J. M. Huxley, C. P. McCoy, J. T. Rademacher and T. E. Rice, *Chem. Rev.*, 1997, **97**, 1515-1566.
8. G. Wulff, *Chem. Rev.*, 2001, **102**, 1-28.
9. L. Ye and K. Mosbach, *Chem. Mater.*, 2008, **20**, 859-868.
10. K. Haupt and K. Mosbach, *Chem. Rev.*, 2000, **100**, 2495-2504.
11. A. Kugimiya and T. Takeuchi, *Biosens. Bioelectron.*, 2001, **16**, 1059-1062.
12. L. Ye and K. Haupt, *Anal. Bioanal. Chem.*, 2004, **378**, 1887-1897.
13. K. D. Shimizu and C. J. Stephenson, *Curr. Opin. Chem. Biol.*, 2010, **14**, 743-750.
14. P. Turkewitsch, B. Wandelt, G. D. Darling and W. S. Powell, *Anal. Chem.*, 1998, **70**, 2025-2030.
15. M. J. Whitcombe, I. Chianella, L. Larcombe, S. A. Piletsky, J. Noble, R. Porter and A. Horgan, *Chem. Soc. Rev.*, 2011, **40**, 1547-1571.
16. S. Shinde, Z. El-Schich, A. Malakpour, W. Wan, N. Dizeyi, R. Mohammadi, K. Rurack, A. Gjørloff Wingren and B. Sellergren, *J. Am. Chem. Soc.*, 2015, **137**, 13908-13912.
17. W. Wan, M. Biyikal, R. Wagner, B. Sellergren and K. Rurack, *Angew. Chem. Int. Ed.*, 2013, **52**, 7023-7027.
18. K. Takeda, A. Kuwahara, K. Ohmori and T. Takeuchi, *J. Am. Chem. Soc.*, 2009, **131**, 8833-8838.
19. T. Takeuchi, T. Mori, A. Kuwahara, T. Ohta, A. Oshita, H. Sunayama, Y. Kitayama and T. Ooya, *Angew. Chem. Int. Ed.*, 2014, **53**, 12765-12770.
20. R. Horikawa, H. Sunayama, Y. Kitayama, E. Takano and T. Takeuchi, *Angew. Chem. Int. Ed.*, 2016, **55**, 13023-13027.
21. G. Wulff, *Angew. Chem. Int. Ed. Engl.*, 1995, **34**, 1812-1832.
22. J. K. Awino and Y. Zhao, *J. Am. Chem. Soc.*, 2013, **135**, 12552-12555.
23. J. K. Awino and Y. Zhao, *Chem. Commun.*, 2014, **50**, 5752-5755.
24. J. K. Awino and Y. Zhao, *Chem.-Eur. J.*, 2015, **21**, 655-661.
25. J. K. Awino and Y. Zhao, *ACS Biomater. Sci. Eng.*, 2015, **1**, 425-430.
26. S. Fa and Y. Zhao, *Chem. Mater.*, 2017, **29**, 9284-9291.
27. S. Fa and Y. Zhao, *Chem. -Eur. J.*, 2018, **24**, 150-158.
28. P. A. Gale, *Coord. Chem. Rev.*, 2003, **240**, 191-221.
29. R. Martínez-Mañez and F. Sancenón, *Chem. Rev.*, 2003, **103**, 4419-4476.
30. S. Goswami, A. Hazra, R. Chakrabarty and H.-K. Fun, *Org. Lett.*, 2009, **11**, 4350-4353.
31. As shown by Fig. S32, however, the different binding affinities did not translate to a difference in direct fluorescence sensing. We suspect that the fluorescence of the naphthyl group was also influenced by a change of local pH induced by the acids. This pH effect probably dominated in MINP₈-Naph, as all the acids caused small and similar changes in the emission of the MINP.
32. X. Zhang, L. Ao, Y. Han, Z. Gao and F. Wang, *Chem. Commun.*, 2018, **54**, 1754-1757.
33. J. K. Awino, R. W. Gunasekara and Y. Zhao, *J. Am. Chem. Soc.*, 2017, **139**, 2188-2191.
34. J. K. Awino, R. W. Gunasekara and Y. Zhao, *J. Am. Chem. Soc.*, 2016, **138**, 9759-9762.
35. R. W. Gunasekara and Y. Zhao, *J. Am. Chem. Soc.*, 2017, **139**, 829-835.

Table of Contents Graphic



Molecular imprinting in micelles followed by covalent modification of the binding pocket yielded fluorescent sensors with precisely constructed binding pockets.